Evaluation of soil erosion and ecological rehabilitation in Loess Plateau region in Northwest China using plutonium isotopes

Zhang, Weichao; Xing, Shan; Hou, Xiaolin

Published in:
Soil & Tillage Research

Link to article, DOI:
10.1016/j.still.2019.04.004

Publication date:
2019

Document Version
Peer reviewed version

Evaluation of soil erosion and ecological rehabilitation in Loess Plateau region in Northwest China using plutonium isotopes

Weichao Zhang[a,e,#], Shan Xing[a,b,#], Xiaolin Hou[a,c,d,f*]

a) State Key Laboratory of Loess and Quaternary Geology, Shaanxi Key Laboratory of Accelerator Mass Spectrometry Technology and Application, Xi'an AMS Center, Institute of Earth Environment, CAS, Xi'an, 710061, China

b) China Institute for Radiation Protection, Taiyuan, 030006, China

c) Technical University of Denmark, Center for Nuclear Technologies, Risø Campus, DK-4000 Roskilde, Denmark

d) CAS Center for Excellence in Quaternary Science and Global Change, Xi'an, 710061, China

e) University of Chinese Academy of Sciences, Beijing, 100049, China

f) Open Studio for Oceanic-Continental Climate and Environment Changes, Pilot National Laboratory for Marine Science and Technology (Qingdao), Qingdao 266061, China

Abstract: Soil erosion is a critical threat to the agriculture and ecosystem in the Chinese Loess Plateau area. Ecological rehabilitation has been applied in large area for reduction of the soil erosion. Six soil depth profiles were collected from Nanxiaohegou watershed

* Corresponding author: *E-mail address*: xiho@dtu.dk (Xiaolin Hou). # S. Xing and W.C. Zhang have same contribution to this paper.

in the Loess Plateau in northwest China and analyzed for the activity concentrations of plutonium isotopes. The measured $^{240}Pu/^{239}Pu$ atomic ratios in all these samples (0.186±0.017) showed that the global fallout was the dominant source of plutonium in this region. An exponential decline of $^{239,240}Pu$ activity concentrations with depth was observed in most of soil profiles. The total inventory of $^{239,240}Pu$ in the reference site was calculated to be 110 Bq/m^2, agreeing well with the reported total fallout value in this latitude. The soil erosion rates were estimated by comparison with the reference site to be 538-941 t/km^2/yr in the most of sites. While an excessive inventory of $^{239,240}Pu$ (186 Bq/m^2) compared to the reference site was observed in one site in the base area, indicating a significant accumulation of soil occurred in this area. The soil erosion depths were estimated to be 2.4-4.6 cm in most of sites during 1963-2016, which can be classified as minor erosion. Compared with the erosion rates in the Nanxiaohegou watershed in 1963-2012 which was estimated by other methods, it is suggested that the natural grass is better for long-term ecological restoration, especially in slope area.

Keyword: $^{239,240}Pu$; soil erosion; ecological rehabilitation; ICP-MS/MS; Loess Plateau

1. Introduction

Soil erosion is one of the severe ecological and environmental challenges worldwide, seriously effecting soil fertility, crop production, water quality ecological system and human survival. More than 60% of Loess Plateau of China with an area of 640,000 km^2 suffers the most severe soil erosion in the world, with soil erosion rates

ranging from 5000 t/km^2/yr to 10000 t/km^2/yr (Cai, 2001; Zhao et al., 2013). In order to reduce soil erosion and achieve sustainable development in the Loess Plateau region, large areas of sloping farmland have been prohibited for cultivation and returned to forest or grassland in northwest China since the 1990s (Chen et al., 2015). It is necessary to evaluate the adaptability and effectiveness of the rehabilitation methods.

The normalized difference vegetation index and soil erosion rate are two indexes often used to evaluate the effectiveness of ecological rehabilitation (Fu et al., 2017). The normalized difference vegetation index is usually obtained by remote sensor monitoring (Larsson, 1993), it mainly presents a short term or current time effectiveness. The erosion rate of soil can provide information regarding long-term impact, so more accurate and effective in the evaluation of the ecological rehabilitation.

Different techniques have been applied for evaluation of the soil erosion rate, such as runoff plots, field survey, positioning method, remote sensing and radionuclides tracer techniques (Fu et al., 2003; Liu et al., 2018; Su et al., 2018; Sepuru and Dube, 2018; Walling et al., 1999; Xu et al., 2015; Zheng et al., 2007). The runoff plots method (Fu et al., 2003) is used to measure the soil erosion rate of a single event. The field survey (Liu et al., 2018) is rough and not reflect the soil erosion in the short term. Although positioning method (Su et al., 2018) can provide the soil erosion rate in small watersheds, it is difficult to evaluate the soil erosion rate in large watersheds. Remote sensing can be used to evaluate soil erosion in large watershed by estimating the land coverage by vegetation, but the derived results are the short-term data and do not

accurately reflect the soil erosion rate (Sepuru and Dube, 2018). Radionuclide tracer technique is a quantitative method for evaluation of soil erosion in both the short- and long- term. This method has been also successfully used to investigate the temporal and spatial variation of soil erosion (Walling et al., 1999; Xu et al., 2015; Zheng et al., 2007).

^{137}Cs, ^{7}Be and ^{210}Pb are the commonly used radionuclide tracers for investigation of soil erosion (Walling et al., 1999; Xu et al., 2015; Zheng et al., 2007). Because of the extremely short half-life of ^{7}Be (53.3 days), it can be only used to investigate soil erosion in a short-term of less one year. ^{210}Pb, a daughter radionuclide of ^{222}Rn, besides being constantly deposited on the soil from the atmosphere, can be also intrinsically formed from the ^{226}Ra (^{238}U) in the soil. In addition, the ^{222}Rn can also escape/migrate from the deep soil, making it more complicated for soil erosion investigation (Branford et al., 2004). Also, the low energy gamma emission of ^{210}Pb (46.5 keV) with low intensity (4.2%) make its sensitive measurement difficult (Branford et al., 2004). Therefore, ^{210}Pb is not commonly used for this purpose. Anthropogenic ^{137}Cs originated from the global fallout of nuclear weapons tests mainly in 1961-1962 has been widely used for investigation of soil erosion in the past decades due to its easy measurement using gamma spectrometry. However, the relatively short half-life (30.2 years) makes the level of the global fallout ^{137}Cs in the soil reduced to about a quarter of initiated value by radioactive decay. The accurate measurement of ^{137}Cs in the soil becomes more difficult, especially for the deep soil (>15 cm), where the ^{137}Cs concentration became too low to be measured by gamma spectrometry. ^{239}Pu and ^{240}Pu are long-lived

84 radionuclides with half-lives of 24 and 6.6 kyr, respectively, and mainly originated from
85 the global fallout of the nuclear weapons tests in the environment. It was reported that
86 plutonium is also highly associated with soil grains when entered into the soil (Zhang
87 et al., 2010), therefore they were suggested as ideal substitutes of ^{137}Cs for investigation
88 of soil erosion (Xu et al., 2015; Zheng et al., 2008). In addition, with the rapid
89 development of mass spectrometry, ^{239}Pu and ^{240}Pu can be easily and sensitively
90 measured using inductively coupled plasma mass spectrometry (ICP-MS) in large
91 number of samples (Xing et al., 2018), making it an attractive radionuclide tracer for
92 investigation of soil erosion.

93 This work aims to assess soil erosion in two catchments with natural vegetation
94 rehabilitation and artificial afforestation rehabilitation in the same region in
95 Nanxiaohegou watershed in the Loess Plateau of northwest China using ^{239}Pu and ^{240}Pu
96 as tracers. This is implemented by determination of activity concentration of ^{239}Pu and
97 ^{240}Pu in 6 soil depth profiles collected in this watershed using extraction
98 chromatography separation of plutonium and ICP-MS/MS measurement of ^{239}Pu and
99 ^{240}Pu. The results are used to evaluate the effectiveness of different ecological
100 rehabilitation methods for reducing soil erosion.
101

2. Materials and Methods

2.1 Study area and soil sampling

Two ecological rehabilitation areas (Dongzhuanggou (DZG) and Yangjiagou (YJG) catchments) in the Nanxiaohegou watershed (35.7 °N, 107.5 °E), located in Loess Plateau in Qingyang, Gansu Province in northwest China (Fig. 1), were selected for investigation of the soil erosion and evaluation of the effectiveness of the different ecological rehabilitation methods in past decades. Nanxiaohegou watershed is a small watershed of 36.5 km^2, located at Xifeng Soil and Water Conservation station managed Huanghe Hydrological Committee, the annual average temperature is 9.3℃ and annual average precipitation rate is 556 mm in this watershed (Chen, 2010; Jin et al., 2018).

DZG and YJG are two adjacent catchments in Nanxiaohegou watershed with a typical hilly–gullied topography of Chinese Loess Plateau. The two catchments are now covered by forest and grass respectively, but were cultivated and planted with crops before 1954. The soil erosion in the Loess Plateau of Northwest China is serious due to soil property of lose and fine grains, extreme precipitation events and extensive land cultivation in this region. The Nanxiaohegou watershed has been used for evaluation of the different methods for rehabilitation since 1954. In the catchment of DZG (1.15 km^2, 1.6×0.72 km), natural vegetation (grass) restoration without human disturbance was applied for ecological rehabilitation of land since 1954. *Agropyron cristatum, Bothriochloa ischaemum, Arundinella hirta, Artemisia argyi* and *Echinochloa crusgalli* are the dominant species of grass in this area. While, an artificial restoration was

adopted in the YJG catchment (0.87 km^2, 1.5×0.58 km) by planting trees in 1954-1958, followed by prohibition for any cultivation until present. *Robinia pseudoacacia, Armeniaca sibirica, Pinus tabulaeformis, Salix matsudana* and *Platycladus orientalis* are the dominant species of shrubs in this artificial forest. The vegetation coverages of DZG and YJG are 65- 90% (Chen, 2010; Jin et al., 2018). The well documented information and different rehabilitation methods in these two catchments in the Nanxiaohegou watershed as a soil and water conservation observation station provide an idea place for this study in Loess Plateau in Northwest China.

Three sites in each catchment of DZG and YJG (Fig. 1) were selected for sampling, i.e. top area (D1/Y1), slope area (D2/Y2) and base area of (D3/Y3). Soil profiles of 40-80 cm in depth were sampled manually, 2.0 cm intervals for the top 30 cm soil and 5.0 cm intervals for the deeper part (>30 cm) were taken in Nov. 2016 using a small stainless steel spade. The collected samples were sealed in plastic bags and transported to the laboratory for analysis. The soil was first weighed and air dried. After removal of the stones (>2mm) and roots of vegetation, the sample was dried in an oven at 150°C for 2-3 days until constant weight. The dried samples were ground and sieved through an 80-mesh sieve.

2.2 Sample analysis

The soil samples were analyzed for plutonium isotopes using radiochemical separation followed by ICP-MS measurement, the detailed analytical method has been

reported elsewhere (Xing et al., 2018). A brief description of the analytical method is presented here: (1) the dried and ground soil samples were first ashed at 450℃ overnight and then leached using *aqua regia* after spiking a known amount of ^{242}Pu; (2) the plutonium isotopes were separated from matrix in the leachate by co-precipitation with iron hydroxides, washing with NaOH, (3) the plutonium isotopes were purified using extraction chromatography with TEVA column after adjust plutonium to Pu (IV); (4) the final separated plutonium sample solution was measured by ICP-MS/MS (Agilent 8800) using NH_3-He as the reaction gas. With this method, the decontamination factor of uranium in the separated plutonium solution is more than 5×10^4, the contribution of uranium at m/z=239 by tailing of $^{238}U^+$ and $^{238}U^1H^+$ in the ICP-MS/MS was measured to be less than 2×10^{-6}, the interference of uranium in soil samples for the determination of low level ^{239}Pu and ^{240}Pu was therefore sufficiently removed.

The measurement sensitivity for ^{239}Pu and ^{240}Pu is 710 cps/ppt and chemical recovery of plutonium is 75-95%, and the estimated detection limits of this method for ^{239}Pu and ^{240}Pu are 0.55 fg/mL for ^{239}Pu and 0.09 fg/mL for ^{240}Pu using the procedure blank. The blank was subtracted from the measured results of samples for calculation of the activity concentrations of plutonium isotopes.2.3 Estimation of the soil erosion rate

The estimation of the soil erosion using $^{239,240}Pu$ is based on that ^{239}Pu and ^{240}Pu in the environment is mainly originated from the global fallout of atmospheric nuclear weapons tests and homogenously deposited in the land of certain area (e.g. band of

similar latitude), and highly associated with soil particles (UNSCEAR, 2000). The inventory of ^{239,240}Pu (reserved) in the soil column will be changed when water or wind erosion or accumulation happened, therefore, the variation of the inventory of plutonium in the soil core directly reflects the loss or accumulation of soil (Xu et al., 2015). By comparing the inventory of ^{239,240}Pu measured in the sampling sites with the measured value in the reference site (no significant loss or accumulation of soil), the erosion or accumulation rate of soil can be estimated. Some models have been proposed for estimate the soil erosion rate and depth using radionuclide tracers, a simple and often used mode for estimation of erosion rate of uncultivated soil using radionuclide (e.g. ^{239,240}Pu) as a tracer was used in this work (Zhang et al. 1999; Walling et al. 2002; Hoo et al., 2011; Lal et al., 2013; Xu et al., 2015)). This model is based on the following four assumptions:

(1) The soil erosion rate in the investigated site is constant during in the study period.

(2) The decay of radionuclide is neglected or can be corrected during the study period. Due to the very long half-lives of ^{239}Pu (2.41×10^4 years) and ^{240}Pu (6.56×10^3 years) compared to the study time span (<100 year), there is no need for decay correction.

(3) The reference site is defined as the site/area where did not disturbed by human activities and no soil erosion or accumulation occurred.

185 (4) The investigated region has the same climate (precipitation rate, wind direction
186 and intensity, temperature, etc.) to ensure the same deposition level of radionuclide
187 tracer.

188 The total inventory of ^{239,240}Pu (I) in a soil column can be calculated using equation
189 (1) (Hoo et al., 2011).

190 $$I = \int_0^Z B f(z)\, dz \quad (1)$$

191 where Z is soil depth (m), B is soil bulk density ($\times 10^{-3}$ t/m^3), $f(z)$ is the inventory of
192 ^{239,240}Pu in a soil interval Z (m).

193 According to the differences between the measured inventories at the sampling
194 site (I_{st}) and reference site (I_{ref}), the loss of ^{239,240}Pu inventory (I_{loss}) due to the soil
195 erosion could be calculated from equation (2) (Hoo et al., 2011; Lal et al., 2013).

196 $$I_{loss} = I_{ref} - I_{st} \quad (2)$$

197 The inventory of ^{239,240}Pu (Bq/m^2) in the soil core exponentially decline with depth
198 in the reference site, and it could be expressed by the equation (3) (Walling et al., 2002).

199 $$C = f(z) = \alpha e^{-\lambda z} \quad (3)$$

200 Where, the coefficients of α and λ could be obtained through exponential fitting of the
201 depth profile of ^{239,240}Pu at the reference site (Fig. 5). Here, λ is the coefficient
202 distributing profile shape of ^{239,240}Pu inventory in the soil core, the smaller the value of
203 the shape factor, the deeper the penetration of plutonium into the soil core; α is the
204 activity concentration of ^{239,240}Pu at z=0 (i.e. top surface of the soil core).

According to the assumption that most of $^{239, 240}$Pu of global fallout input in soils was received in 1963 (Zhang et al., 1999), the thickness of the lost soil (L(cm)) at the sampling site since 1963 can be calculated using the equation (4) (Hoo et al., 2011).

$$L = - \frac{\ln(1-\frac{I_{loss}}{I_{ref}})}{\lambda} \times 100 \quad (4)$$

Then, the average soil erosion rate, E (t/km^2/yr) since 1963 could be estimated using equation (5) (Zhang et al., 1999).

$$E = \frac{10BL}{T-1963} \quad (5)$$

Where, B is the soil bulk density ($\times 10^{-3}$ t/m^3), L is the thickness of the lost soil ($\times 10^{-2}$ m), and T is the sampling date (year).

3 Results and discussion

3.1 Distribution of ^{239,240}Pu activity concentrations and inventories in the soil profiles from DZG and YJG catchments

The ^{239,240}Pu activity concentrations in the surface soil (0-4 cm) at the top area in the soil profiles D1 and Y1 range from 0.304±0.026 mBq/g to 1.20±0.07 mBq/g (Fig. 2 and Fig. 3), which close to the reported ranges of (0.466-1.62) mBq/g in the same latitudes (Xu et al., 2015). ^{239,240}Pu activity concentration in 0-2 cm depth at site D1 (1.20 mBq/g) is three times higher than that at site Y1 (0.304 mBq/g). The inventories of ^{239,240}Pu at the sites D1 and Y1 are calculated to be 111±5 Bq/m^2 and 72.9±3.7 Bq/m^2, respectively, which are similar to the values reported in Beijing (107 Bq/m^2), Dalian (84.5-90.0 Bq/m^2) and Chengde (138 Bq/m^2) in the similar latitude in China (Dong,

2010; Ni et al., 2018; Xu et al., 2015). It can be observed that the ^{239,240}Pu activity concentrations in soil column at site D1 decrease exponentially with the increased depth, while the ^{239,240}Pu activity concentrations in soil column at site Y1 show almost uniform distribution in the upper 12 cm and followed by an exponential decrease (Fig. 2). The large difference of ^{239,240}Pu activity concentration distribution and inventory between sites D1 and Y1 is related to the different sampling environment and disturbance. Compared to the sampling site of D1 with the flat terrain and higher vegetation coverage (90%) and without obvious disturbance as well as potential soil accumulation or erosion, the soil profile of Y1 might be disturbed and suffered erosion.

In the slope area (D2/Y2), the highest ^{239,240}Pu activity concentrations are 1.01±0.08 mBq/g at the site D2 and 0.444±0.053 mBq/g at the site Y2, which are lower than that at site D1 (1.20±0.07 mBq/g) (Fig. 2 and Fig. 3). The estimated inventories of ^{239,240}Pu at site D2 (53.5±2.1 Bq/m^2) and Y2 (56.5±3.1 Bq/m^2) are about half of the inventory at site D1 (111 Bq/m^2). This should results from the fact that the surface soil is easily lost at the slope (>25°) area by rainfall runoff, especially in the case of heavy rain. It was observed that the highest ^{239,240}Pu activity concentration at D2 occurs in the top soil (0-2 cm), while at the site of Y2, the highest value occurs in the subsurface layer in the depth of 8-10 cm, indicating a different extent of soil erosion/accumulation at two sites. In the early stage of ecological rehabilitation, the vegetation (grass) coverage of the land for the natural rehabilitation by native grass is higher than that for artificial rehabilitation by planting trees due to the rapid growth rate of the grass. As a

result, a higher loss of the upper soil (0-8 cm) at Y2 happened compared to only the top soil (0-2 cm) at D2 due to the water and wind erosion. The lower value of the maximum ^{239,240}Pu activity concentration and low total inventory of ^{239,240}Pu at site Y2 indicate a significant soil erosion occurred at this site, while the increased $^{239,\ 240}$Pu activity concentrations with depth in the upper 8 cm soil at site Y2 might imply that there is an accumulation of the low ^{239,240}Pu soil originated from the upper part in this catchment at this site.

In the base area (D3/Y3), the highest ^{239,240}Pu activity concentrations are 0.905±0.084 mBq/g at D3 and 0.990±0.149 mBq/g at Y3 (Fig. 2 and Fig. 3), also lower than that at the site D1 (1.20 mBq/g). The estimated inventories of ^{239,240}Pu are 75.4±2.5 Bq/m^2 at site D3 and 186±4 Bq/m^2 at Y3. Compared to the site D1, a lower inventory of ^{239,240}Pu (75.4 Bq/m^2) at D3 indicates that the soil erosion occurred also at this site (D3). Although this site is located in the base area of this catchment, but not flat instead with a slope of >20°, causing a loss of the surface soil by wind and runoff of the precipitation. The inventory of ^{239,240}Pu (186 Bq/m^2) at site Y3 is higher than that at reference site D1 (111 Bq/m^2), indicating an extra input of ^{239,240}Pu associated particles (soil) occurred in this base area. Based on the results that most of the plutonium (>95%) presents in the upper 22 cm soil layer at D1 and Y1 sites in this region, the inventories of ^{239,240}Pu at the site Y3 are estimated to be 89.6 Bq/m^2 in the layer of 0-22 cm and 96.7 Bq/m^2 in the deep soil (> 22 cm), showing 52% of plutonium presents in the deep layer (>22 cm). These results imply that a significant accumulation of soil occurred in

the base area (Y3) in the YJG catchment, and the upper layer (0-22 cm) soil with low activity concentration of ^{239,240}Pu might originated from the erosion of soil in the slope area in the early stage of ecological rehabilitation in the YJG catchment.

3.2 Source of plutonium isotopes in Nanxiaohegou watershed

The measured ^{240}Pu/^{239}Pu atomic ratios (Fig. 4) are similar and distributed in a narrow range of 0.142-0.227 with an average of 0.186±0.017 in all 6 soil depth profiles. These values agree well with that of global fallout (0.178±0.023) (Kelley et al., 1999), but are significantly different with those in the nuclear weapons (0.01-0.07) (Chiappini et al., 1999; Wolf et al., 1997) and releases from nuclear power plants (0.23-0.67) (Warneke et al., 2002). These results suggest that plutonium in the soil profiles in this region mainly originated from the global fallout of the nuclear weapons tests.

The Chernobyl nuclear accident in 1986 released large amount of radioactive substances to the environment, but most of them were dispersed and deposited in the local region and some parts of Europe (Levi, 1991; Muramatsu et al., 2000). Although very low level ^{131}I and ^{137}Cs released from Chernobyl accident were measured in China, no measured Chernobyl-derived plutonium was reported in China, since plutonium is not volatile element, a small amount of plutonium released as relative bigger particles during Chernobyl accident was mainly deposited in nearby areas. A small signal of Chernobyl derived plutonium was measured in the aerosol samples collected during the accident in Japan, but very small compared to the releases from the atmospheric nuclear

289 weapons tests (Hirose et al. 2001). The Fukushima accident in 2011 also released large
290 amounts of radioactive substances into the air, but only low levels of volatile ^{131}I and
291 ^{137}Cs from the Fukushima accident were detected in China because of the dominant
292 westwards wind during the accident. It was reported that very small amount of
293 plutonium was released from the Fukushima accident, and Fukushima derived
294 plutonium was observed only in some samples in the 20 km area of the Fukushima
295 Daiichi NPP. No plutonium from Fukushima was observed in other regions including
296 China (Zheng et al., 2013). In addition, the $^{240}Pu/^{239}Pu$ atomic ratio in the fallout from
297 the accident in Chernobyl (0.386-0.412) (Boulyga et al., 1997; Wendt et al., 1999) and
298 Fukushima (0.323-0.330) (Zheng et al., 2013) are much higher than the measured
299 values in this work, therefore, the contribution of plutonium in the studied region from
300 these two nuclear accidents can be excluded.
301 In addition, the studied region is far away from the sites of nuclear weapons tests,
302 the nearest test site at Lop Nor is located about 1700 km northwest of the sampling
303 region. Although the sampling site is located in the downwind direction, but it is too far
304 to receive close-in deposition of the nuclear weapons tests conducted in this site in
305 1964-1980. There is no nuclear facility in the sampling region, the nearest facility
306 (reprocessing plant in Jiayuguan) is located 950 km north of the sampling region. A
307 relative lower $^{240}Pu/^{239}Pu$ ratio of 0.158 (in average) was reported in soil samples
308 collected in Jiuquan region 300-500 km east of Lop Nor, which was attributed to more
309 than 40% contribution from the Chinese Nuclear weapons tests in Lop Nor. (Bu et al.

2015). While, the investigations in the north China do not show obvious close-in deposition of plutonium in large area of 500-2000 km distance to this nuclear weapons test site and reprocessing facility in Jiayuguan, and similar $^{240}Pu/^{239}Pu$ ratios as global fallout were reported in the soil from Lanzhou (0.188±0.009) (Zheng et al., 2009), Zhongxiang (0.186±0.008) and Xiangyang (0.198±0.006) (Dong, 2010), as well as sediment from Lake Hongfeng (0.185±0.009) (Zheng et al., 2008) and Lake Poyang (0.187±0.004) (Liao et al., 2008) in China. This supports that the dominant source of plutonium isotopes in the study region is the global fallout of nuclear weapons tests before 1980. Therefore, plutonium in this region is suitable for soil erosion investigation.

3.3 Selection of reference site

Two soil cores (D1 and Y1) were collected on the top of the two catchments. The sampling site D1 on the top of the DZG catchment is located in a flat area without visible disturbance, and is well covered by grass. The distribution of $^{239,240}Pu$ in this soil core (Fig. 2 and Fig. 3) shows an exponentially declining trend with increased depth, and the highest activity concentration was observed in the top layer. This suggests that there is no disturbances in this area, at least since 1963 when the major global fallout occurred. The most plutonium (>95%) in the soil core was found in the top 10 cm, indicating a very slow migration of plutonium since its deposition on the land. This might be attributed to the strong association/binding of plutonium with the soil particles

(Zhang et al., 2010). Soil in Nanxiaohegou watershed contain high silt (67-74%), but not high organic matter content (0.7-1.4%). The soil particles in watershed are quick small (<0.5 mm) (Guo et al. 2018). It has been reported that the fallout plutonium is mainly associated with fine particles and organic substances in soil, and the mobile species of plutonium (water soluble or exchangeable fractions) in soil account for a very small fraction (Qiao et al., 2012).

The total inventory of ^{239,240}Pu in the soil core at site D1 is calculated to be 111 Bq/m^2 by summing up ^{239}Pu + ^{240}Pu in all intervals of the entire soil profile. This value agrees well with the reported global fallout of plutonium (^{239,240}Pu) in the similar latitude, e.g. Lake Erie (~42°N) in America (108 Bq/m^2) (Ketterer et al., 2002), Euiwang (~37°N) in South Korea (102Bq/m^2) (Lee et al., 1996), and Dalian (~39°N) (84.5-90.0Bq/m^2) (Xu et al., 2015). The variation of the total inventory in these site might attributed to the different climate condition, e.g. precipitation rate. Considering the declining trend of ^{239,240}Pu inventories with depth (Fig. 2), this feature indicates that there has been no significant erosion and accumulation of soil in this area. Therefore, this site can be used as the reference site for the evaluation the soil erosion in this watershed.

Fig. 5 shows the distribution of the inventories of ^{239,240}Pu in each interval of soil profile with the depth, a declining trend from 31.2Bq/m^2 in the top layer to 0.1Bq/m^2 in the bottom layer is observed. The fitting analysis shows an exponentially declining formula of $I_{pu} = 3.58e^{-0.159z}$ with a correlation factor of 0.93.

For the profile at site Y1 (Fig. 2 and Fig. 3), the inventories and activity concentrations of $^{239.240}$Pu in each interval show a relative constant value in the depth of 0-14 cm, indicating that the site Y1 has probably suffered a significant disturbance, and not suitable to be used as a reference site. Therefore, the D1 is selected as the reference site for both catchments in the Nanxiaohegou watershed.

3.4 Estimation of the rate, depth and intensity of soil erosion in the Nanxiaohegou watershed

The rate and depth of soil erosion are calculated according to the equations of (1) - (5), the results (Table 1) show that the soil erosion rate ranges from 538 to 941 t/km^2/yr, and the erosion depths range from 2.4 to 4.6 cm in all sites except Y3. These results agree well with the reported soil erosion rate (290-725t/km^2/yr) and erosion depth (1.06-2.65 cm) in the other areas in the Nanxiaohegou watershed estimated using ^{137}Cs as tracer (Wu and Kou, 1997). At the site Y3, a negative value of -719 t/km^2/yr for erosion rate and -3.3 cm for erosion depth are calculated, indicating a soil accumulation occurred in this area. This results from that the site Y3 is located in the base area of the YJG catchment, and the eroded soil from the slope was transported and piled up in this area due to its relative flat topography. It should be noted that the calculated negative values for erosion rate and erosion depth could not be used to estimate the level of the accumulation, because the formulas for calculation of erosion rate and depth are not valid in the case of soil accumulation.

373 The estimated erosion rate in the sites of D2, D3, Y1, Y2 and D3 are less than 1000
374 t/km^2/yr, which can be classified to be minor erosion according the criteria of
375 classification and gradation of soil erosion (SL190-2007) in China (SL190-2007, 2007).
376
377 **3.5 Evaluation of the different rehabilitation methods for reducing soil erosion**
378 The results in this work show a similar soil erosion rate in two catchments using
379 different ecological rehabilitation methods (Table 1). This might indicate that both
380 rehabilitation methods are effective in the reduction of soil erosion.
381 As an experimental field for evaluation of ecological rehabilitation methods, soil
382 erosion rate in the Nanxiaohegou watershed was routinely monitored by measuring the
383 amount of soil collected after each precipitation using V-shaped runoff gathering pit,
384 which was embedded into the soil of base area. Table 2 shows the estimated values of
385 soil erosion rates in DZG and YJG catchments with the corresponding precipitation rate
386 in different periods (Chen, 2010; Li, 2006; Yuan et al., 2014). The reported erosion
387 rates by collecting the soil in the base area are only attributed to the water erosion, and
388 no wind erosion is included, because they were measured after each precipitation event.
389 With the reported data (Chen, 2010; Li, 2006; Yuan et al., 2014), the soil erosion
390 rates in the DZG and YJG catchments in different stages can be calculated and
391 compared (Table 2). In the early stage of ecological rehabilitation (1954-1962), high
392 soil erosion rate was observed in the DZG catchment (4611 t/km^2/yr), which is
393 classified as heavy erosion. The erosion rate in the YJG catchment (1280 t/km^2/yr) was

394 3.6 times lower in this period, can classified as major erosion. A significantly decreased
395 soil erosion rate in the DZG (3000 t/km^2/yr) in 1963-2012 was observed. An even more
396 significant reduction of soil erosion rate by a factor of about 2.8 was observed in the
397 catchment of YJG (454 t/km^2/yr) during the same period. This confirms that both
398 ecological rehabilitation methods are effective in the reduction of soil erosion rate, and
399 more rapid reduction of soil erosion occurred in YJG than that in DZG. The estimated
400 soil erosion rate using ^{239,240}Pu as tracer in this work in the period of 1963-2016 agrees
401 well with the previously reported values in the literatures (Chen, 2010; Li, 2006; Yuan
402 et al., 2014) using the conventional method in the YJG catchment. But much lower
403 values (538-964 t/km^2/yr) in the DZG catchment in 1963-2016 were estimated in this
404 work compared to the reported value (3000 t/km^2/yr) in 1963-2012, using a
405 conventional method based on the measurement of the eroded soil in each single
406 precipitation event. The results estimated using ^{239,240}Pu in this work reflect an
407 integrated erosion, which might be more accurate for evaluation the effectiveness of the
408 ecological rehabilitation method. Based on this data, the reduction of soil erosion in the
409 DZG catchment using natural vegetation rehabilitation is also very effective, and from
410 a heavy erosion with an erosion rate of 4611 t/km^2/yr in 1954-1962 to a minor erosion
411 with erosion rate of 538-941 t/km^2/yr in 1963-2016.

412 This result agrees well with the previous investigations in this region (Fu et al.,
413 2009; Li et al., 2009). The much lower soil erosion rate in the late stage compared to
414 the early stage of the ecological rehabilitation was observed, especially for the DZG

415 catchment where natural vegetation rehabilitation was applied since 1954. This
416 indicates that mature forest and grass are better in reducing soil erosion than young
417 forest and crops (Fu et al., 2009; Li et al., 2009).

418 The effectively suppressed soil erosion by two ecological rehabilitation methods
419 might result from that the soil erosion by rainfall splashing due to the kinetic energy of
420 rain drops was well reduced by vegetation coverage with forest and grass (Fu et al.,
421 2009). Besides, the vegetation is helpful for the preservation of soil grains and water,
422 and in return helps long survival time of the vegetation. The root density also plays an
423 important role in reducing soil erosion because of the effect of enlacing and absorption
424 between root exudates and soil particles (Li et al., 2014). As a consequence, the soil
425 erosion rate was significantly reduced from the first stage to the late stage of ecological
426 rehabilitation.

427 Compared to the reduction of erosion rate in the DZG and YJG catchments in the
428 same period (Table 2), it can be seen that artificial rehabilitation by planting trees/forest
429 in the YJG catchment is superior to natural vegetation rehabilitation with the grass in
430 the DZG catchment in short-time scale. This also agrees with the previous report (Fu et
431 al., 2009; Jin et al., 2018; Li et al., 2009). Investigations using ^{137}Cs tracer in other
432 Loess Plateau and Sichuan basin in China have shown that the soil erosion rate in the
433 mature forest is lower than that in the grassland (Fu et al., 2009; Li et al., 2009). A soil
434 erosion rate measurement using the runoff plots method in Ansai, China in 2003 in
435 single precipitation event showed that the average erosion rate in each precipitation

436 event in the grass rehabilitated land (4.6 t/km^2) is two times higher than that in the
437 artificial forest rehabilitated land (1.0-2.6 t/km^2) (Zhao et al., 2006). This was attributed
438 to the kinetic energy of rainfall (drops), which can be highly reduced by the resistance
439 of the forest when it drops to the soil surface (Fu et al., 2009). In addition, the forest
440 can also reduce the intensity of the wind, therefore reducing the soil erosion by wind.
441 Comparing the reduction of the soil erosion rates in the DZG and YJG catchments
442 between the periods of 1954-1962 and 1963-2012, it can be found that the reduction of
443 the erosion rates in the DZG catchment (1608 t/km^2/yr) is two times higher than that in
444 the YJG catchment (825 t/km^2/yr) (Chen, 2010; Li, 2006; Yuan et al., 2014). This result
445 might suggested that the natural rehabilitation is a more suitable method of ecological
446 rehabilitation compared to the artificial rehabilitation in a long-time scale in this
447 watershed. This might be attributed to the high coverage of the land by the vegetation
448 with increased root density of grass and enlacing and absorption between root exudates
449 and soil particles (Jiang et al., 2016; Li et al., 2014). It should be noted that this
450 conclusion was obtained based on the work in such a small watershed, which might not
451 precisely suitable as a general conclusion. Whether planting trees or seeding grass
452 should be depended on landform condition, generally seeding grass is better for slope
453 area and planting tree for gullies.

454 The slightly higher soil erosion rate in the YJG catchment (551-845 t/km^2/yr, with
455 an average of 698 t/km^2/yr) estimated in this work using ^{239,240}Pu compared to the
456 reported value (454 t/km^2/yr) in 1963-2012 estimated by runoff plot might be attributed

457 to the fact that the erosion rate estimated by ^{239,240}Pu tracer in this work is an integrated
458 value including wind erosion, but the value estimated by runoff plot is only for water
459 erosion. In the early stage of ecological rehabilitation, wind erosion might be significant
460 because the ground is bare. As a result, the difference of 244 t/km^2/yr should be mainly
461 attributed to wind erosion.
462
463 **4. Conclusions**
464 Based on the results and discussion above, it can be concluded: 1) the dominant
465 source of ^{239,240}Pu in the investigated region in the Nanxiaohegou watershed in the
466 Chinese Loess Plateau is global fallout; 2) more than 80% of ^{239,240}Pu is present in upper
467 14 cm layer in the most of the soil cores, and the total inventory of ^{239,240}Pu (110 Bq/m^2)
468 at the reference site with no significant erosion and accumulation agrees well with the
469 reported values in other areas in the same latitude; 3) the plutonium isotopes as an ideal
470 tracer was successfully applied to evaluate of soil erosion and ecological rehabilitation
471 in Loess Plateau region in Northwest China, the soil erosion rates of 538-941 t/km^2/yr
472 and erosion depth of 2-5 cm were estimated in most of the areas, which are classified
473 as minor erosion, except a site in the base area where a significant accumulation was
474 observed; 4) both natural vegetation rehabilitation and artificial tree planting
475 rehabilitation are effective for reducing the soil erosion; the natural rehabilitation shows
476 more adaptive for long term ecological rehabilitation, especially in slope area.
477

Acknowledgments

This work was supported by the National Natural Science Foundation of China (11605206, 11875261, and 41603125), the Ministry of Science and Technology of China (2015FY110800), National Research Program for Key Issues in Air Pollution Control (DQGG0105-02) and Chinese Academy of Sciences (132B61KYSB20180003). The authors appreciate the constructive comments from the three anonymous referees.

References:

Boulyga, S.F., Erdmann, N., Funk, H., Kievets, M.K., Lomonosova, E.M., Mansel, A., Trautmann, N., Yaroshevich, O.I., Zhu, I.V., 1997. Determination of isotopic composition of plutonium in hot particles of the Chernobyl area. Radiat. Meas. 28, 349-352. https://doi.org/10.1016/S1350-4487(97)00098-X.

Branford, D., Fowler, D., Moghaddam, M.V., 2004. Study of Aerosol Deposition at a Wind Exposed Forest Edge Using ^{210}Pb and ^{137}Cs Soil Inventories. Water, Air and Soil Pollut. 157, 107-116. https://doi.org/10.1023/B:WATE.0000038879.99600.69.

Bu, W., Ni, Y., Guo, Q., Zheng, J., Uchida, S., 2015. Pu isotopes in soils collected downwind from Lop Nor: regional fallout vs. global fallout. Sci. Rep. 5, 12262. https://doi.org/10.1038/srep12262.

Cai, Q., 2001. Soil erosion and management on the Loess Plateau. J. Geogr. Sci. 11, 53-70. https://doi.org/10.1007/BF02837376.

Chen, P., 2010. A study on influences of land use pattern changing on soil and water loss in small watershed of Loess Plateau gully region. Beijing Forestry University (in Chinese).

Chen, Y., Wang, K., Lin, Y., Shi, W., Song, Y., He, X., 2015. Balancing green and grain trade. Nat. Geosci. 8, 739-741. https://doi.org/10.1038/ngeo2544.

Chiappini, R., Pointurier, F., J.C.Millies-Lacroix, Lepetit, G., Hemet, P., 1999. $^{240}Pu/^{239}Pu$ isotopic ratios and $^{239+240}Pu$ total measurements in surface and deep waters around Mururoa and Fangataufa atolls compared with Rangiroa atoll (French Polynesia). Sci. Total Environ. 237-238, 269-276. https://doi.org/10.1016/S0048-9697(99)00141-2.

Dong, W., 2010. Distribution and Behavior of Pu Isotopes in the Environment. Peking University. (in Chinese).

Fu, B., Wang, S., Liu, Y., Liu, J., Liang, W., Miao, C., 2017. Hydrogeomorphic Ecosystem Responses to Natural and Anthropogenic Changes in the Loess Plateau of China. Annu. Rev. Earth Planet. Sci. 45, 223-243. https://doi.org/10.1146/annurev-earth-063016-020552.

Fu, B., Wang, Y., Lu, Y., He, C., Chen, L., Song, C., 2009. The effects of land-use combinations on soil erosion: a case study in the Loess Plateau of China. Prog. Phys. Geogr. 33, 793-804. https://doi.org/10.1177/0309133309350264.

517 Fu, S., Fu, J., Wang, X., Liu, B., Yuan, A., 2003. Sediment Content Measurement in
518 Collecting Tanks of Runoff Plots. Bull. Soil Water Conserv. (in Chinese). 23, 39-
519 41. https://doi.org/10.13961/j.cnki.stbctb.2003.06.011.
520 Guo, M.M., Wang, W.L., Kang, H.L., Yang, B., 2018. Changes in soil properties and
521 erodibility of gully head induced by vegetation restoration on the Loess Plateau,
522 China. J. Arid Land. 10(5), 712-725. https://doi.org/10.1007/s40333-018-0121-z
523 Hirose, K., Igarashi, Y., Aoyama, M., Miyao, T., (2001). Long-term trends of
524 plutonium fallout observed in Japan. in Radioactivity in the Environment, Vol 1.
525 2001, 251-266. https://doi.org/10.1016/S1569-4860(01)80018-8
526 Hoo, W.T., Fifield, L.K., Tims, S.G., Fujioka, T., Mueller, N., 2011. Using fallout
527 plutonium as a probe for erosion assessment. J. Environ. Radioact. 102, 937-942.
528 https://doi.org/10.1016/j.jenvrad.2010.06.010.
529 Jiang, W., Yang, S., Yang, X., Gu, N., 2016. Negative impacts of afforestation and
530 economic forestry on the Chinese Loess Plateau and proposed solutions. Quat. Int.
531 399, 165-173. https://doi.org/10.1016/j.quaint.2015.04.011.
532 Jin, Z., Guo, L., Lin, H., Wang, Y., Yu, Y., Chu, G., Zhang, J., 2018. Soil moisture
533 response to rainfall on the Chinese Loess Plateau after a long-term vegetation
534 rehabilitation. Hydrol. Process. 32, 1738-1754. https://doi.org/10.1002/hyp.13143.
535 Kelley, J.M., Bond, L.A., Beasley, T.M., 1999. Global distribution of Pu isotopes and
536 ^{237}Np. Sci. Total Environ. 237-238, 483-500. https://doi.org/10.1016/S0048-
537 9697(99)00160-6.

538 Lal, R., Tims, S.G., Fifield, L.K., Wasson, R.J., Howe, D., 2013. Applicability of ^{239}Pu
539 as a tracer for soil erosion in the wet-dry tropics of northern Australia. Nucl. Instrum.
540 Meth. Phys. Res. B. 294, 577-583. https://doi.org/10.1016/j.nimb.2012.07.041.
541 Larsson, H., 1993. Linear regressions for canopy cover estimation in Acacia
542 woodlands using Landsat-TM, -MSS and SPOT HRV XS data. Int. J. Remote
543 Sensing. 14, 2129-2136. https://doi.org/10.1080/01431169308954025.
544 Levi, H.W., 1991. Radioactive deposition in Europe after the Chernobyl accident and
545 its long-term consequences. Ecol. Res. 6, 201-216.
546 https://doi.org/10.1007/bf02347162.
547 Li, M., 2006. The influence of vegetation change on hydrologic factor in nanxiaohegou.
548 Xi'an University of Technology (in Chinese).
549 Li, M., Li, Z., Yao, W., Liu, P., 2009. Estimating the erosion and deposition rates in a
550 small watershed by the ^{137}Cs tracing method. Appl. Radiat. Isot. 67, 362-366.
551 https://doi.org/10.1016/j.apradiso.2008.10.011.
552 Li, Q., Liu, G.-b., Xu, M., Zhang, Z., 2014. Relationship of Soil Erodibility, Soil
553 Physical Properties, and Root Biomass with the Age of caragana Korshinskii Kom.
554 Plantations on the Hilly Loess Plateau, China. Arid Land Res. Manag. 28, 311-324.
555 https://doi.org/10.1080/15324982.2013.855957.
556 Liao, H., Zheng, J., Wu, F., Yamada, M., Tan, M., Chen, J., 2008. Determination of
557 plutonium isotopes in freshwater lake sediments by sector-field ICP-MS after

separation using ion-exchange chromatography. Appl. Radiat. Isot. 66, 1138-1145. https://doi.org/10.1016/j.apradiso.2008.01.001.

Liu, B., Liu, G., Wang, D.a., Wu, Y., Duan, X., Li, J., Shen, B., Meng, L., Gao, Y., 2018. A field survey method for regional gully erosion: A case study in northeastern China. Sci. Soil Water Conserv. (in Chinese). 16, 34-40. https://doi.org/10.16843/j.sswc.2018.04.005.

Muramatsu, Y., Rühm, W., Yoshida, S., Tagami, K., Uchida, S., Wirth, E., 2000. Concentrations of ^{239}Pu and ^{240}Pu and Their Isotopic Ratios Determined by ICP-MS in Soils Collected from the Chernobyl 30-km Zone. Environ. Sci. Technol. 34, 2913-2917. https://doi.org/10.1021/es0008968.

Ni, Y., Wang, Z., Guo, Q., Zheng, J., Li, S., Lin, J., Tan, Z., Huang, W., 2018. Distinctive distributions and migrations of $^{239+240}$Pu and ^{241}Am in Chinese forest, grassland and desert soils. Chemosphere. 212, 1002-1009. https://doi.org/10.1016/j.chemosphere.2018.09.021.

Qiao, J., Hansen, V., Hou, X., Aldahan, A., Possnert, G., 2012. Speciation analysis of ^{129}I, ^{137}Cs, ^{232}Th, ^{238}U, ^{239}Pu and ^{240}Pu in environmental soil and sediment. Appl. Radiat. Isot. 70, 1698-1708. https://doi.org/10.1016/j.apradiso.2012.04.006.

Sepuru, T.K., Dube, T., 2018. An appraisal on the progress of remote sensing applications in soil erosion mapping and monitoring. Remote Sens. Appl.: Soc. Environ. 9, 1-9. https://doi.org/10.1016/j.rsase.2017.10.005.

SL190-2007, 2007. Standards of classification and gradation of soil erosion. Ministry of Water Resources of the People's Republic of China (in Chinese). China.

Su, Z.a., Xiong, D., Zhang, J., Dong, Y., Yang, C., Zhang, X., Xian, J., 2018. Research progress of soil erosion of purple soil slope farmland and its prevention and control measures. Soil Water Conserv. China. 42-47+69. https://doi.org/10.14123/j.cnki.swcc.2018.0043.

UNSCEAR, 2000. Sources and effects of ionizing radiation. Report to the General Assembly, with Scientific Annexes. Volume II: Effects. United Nations, New York. pp.156-160.

Walling, D.E., He, Q., Appleby, P.G., 2002. Conversion models for use in soil-erosion, soil-redistribution and sedimentation investigations, In: Zapata, F. (Ed.) Handbook for the assessment of soil erosion and sedimentation using environmental radionuclides, Kluwer Ac. Publ., Dordrecht,The Netherlands. pp. 111-164.

Walling, D.E., He, Q., Blake, W., 1999. Use of ^{7}Be and ^{137}Cs measurements to document short- and medium-term rates of water-induced soil erosion on agricultural land. Water Resour. Res. 35, 3865-3874. https://doi.org/10.1029/1999WR900242.

Warneke, T., Croudace, I.W., Warwick, P.E., Taylor, R.N., 2002. A new ground-level fallout record of uranium and plutonium isotopes for northern temperate latitudes. Earth Planet. Sci. Lett. 203, 1047–1057. https://doi.org/10.1016/S0012-821X(02)00930-5.

599 Wendt, K., Blaum, K., Bushaw, B.A., Grüning, C., Horn, R., Huber, G., Kratz, J.V.,
600 Kunz, P., Müller, P., Nörtershäuser, W., Nunnemann, M., Passler, G., Schmitt, A.,
601 Trautmann, N., Waldek, A., 1999. Recent developments in and applications of
602 resonance ionization mass spectrometry. Anal. Bioanal. Chem. 364, 471-477.
603 https://doi.org/10.1007/s002160051370.
604 Wolf, S.F., Bates, J.K., Buck, E.C., Dietz, N.L., Fortner, J.A., Brown, N.R., 1997.
605 Physical and Chemical Characterization of Actinides in Soil from Johnston Atoll.
606 Environ. Sci. Technol. 31, 467-471. https://doi.org/10.1021/es960295+.
607 Wu, Y., Kou, Q., 1997. The method of ^{137}Cs to study soil erosion in the loess gully
608 area of east gansu province. Bull. Soil Water Conserv. (in Chinese). 17, 7-10.
609 https://doi.org/10.13961/j.cnki.stbctb.1997.05.002.
610 Xing, S., Zhang, W., Qiao, J., Hou, X., 2018. Determination of ultra-low level
611 plutonium isotopes (^{239}Pu, ^{240}Pu) in environmental samples with high uranium.
612 Talanta. 187, 357-364. https://doi.org/10.1016/j.talanta.2018.05.051.
613 Xu, Y., Qiao, J., Pan, S., Hou, X., Roos, P., Cao, L., 2015. Plutonium as a tracer for
614 soil erosion assessment in northeast China. Sci. Total Environ. 511, 176-185.
615 https://doi.org/10.1016/j.scitotenv.2014.12.006.
616 Yuan, J., Zhang, F., Li, H., Gao, W., 2014. Law of soil and water loess under different
617 measures in south xiaogehou watershed. Bull. Soil Water Conserv. (in Chinese). 34,
618 39-43. https://doi.org/10.13961/j.cnki.stbctb.2014.03.009.

Zhang, X.B., Walling, D.E., He, Q., 1999. Simplified mass balance models for assessing soil erosion rates on cultivated land using caesium-137 measurements. Hydrol. Sci. J. 44, 33-45. https://doi.org/10.1080/02626669909492201.

Zhang, Y., Zheng, J., Yamada, M., Wu, F., Igarashi, Y., Hirose, K., 2010. Characterization of Pu concentration and its isotopic composition in a reference fallout material. Sci. Total Environ. 408, 1139-1144. https://doi.org/10.1016/j.scitotenv.2009.11.058.

Zhao, G., Mu, X., Wen, Z., Wang, F., Gao, P., 2013. Soil erosion, conservation, and eco-environment changes in the Loess Plateau of China. Land Degrad. Dev. 24, 499-510. https://doi.org/10.1002/ldr.2246.

Zhao, H., Liu, G., Cao, Q., Wu, R.j., 2006. Influence of different land use types on soil erosion and nutrition care effect in loess hilly region. J. Soil Water Conserv. (in Chinese). 20, 20-24, 54. https://doi.org/10.13870/j.cnki.stbcxb.2006.01.005.

Zheng, J., He, X., Walling, D., Zhang, X., Flanagan, D., Qi, Y., 2007. Assessing Soil Erosion Rates on Manually-Tilled Hillslopes in the Sichuan Hilly Basin Using ^{137}Cs and $^{210}Pb_{ex}$ Measurements. Pedosphere. 17, 273-283. https://doi.org/10.1016/S1002-0160(07)60034-4.

Zheng, J., Tagami, K., Uchida, S., 2013. Release of Plutonium Isotopes into the Environment from the Fukushima Daiichi Nuclear Power Plant Accident: What Is Known and What Needs to Be Known. Environ. Sci. Technol. 47, 9584-9595. https://doi.org/10.1021/es402212v.

Zheng, J., Wu, F., Yamada, M., Liao, H., Liu, C., Wan, G., 2008. Global fallout Pu recorded in lacustrine sediments in Lake Hongfeng, SW China. Environ. Pollut. . 152, 314-321. https://doi.org/10.1016/j.envpol.2007.06.027.

Zheng, J., Yamada, M., Wu, F., Liao, H., 2009. Characterization of Pu concentration and its isotopic composition in soils of Gansu in northwestern China. J. Environ. Radioact. 100, 71-75. https://doi.org/10.1016/j.jenvrad.2008.10.017.

661

662 **Caption of the figures**

663

664 Fig. 1 sampling sites in the DZG and YJG in Nanxiaohegou watershed in the loess
665 plateau in northwest China. The elevations of the top catchments and the height
666 from the base to the top area are 1271m and 127 m for YJG and 1305 m and
667 160m in DZG, the slopes of two catchments are 35□ for YJG and 25□ for
668 DZG (slope of the sampling sites at slope); the distances among top-slope and
669 slope-base sampling sites are 250 m and 100 m in YJG and 200 m and 150 m
670 for DZG catchment.

671 Fig. 2 Depth distributions of ^{239,240}Pu activity concentrations in six soil profiles

672 Fig. 3. Depth distributions of ^{239,240}Pu inventories in six soil profiles

673 Fig. 4 Depth distributions of the ^{240}Pu/^{239}Pu atomic ratios in the sampling sites

674 Fig. 5 Depth distributions of $^{239,\ 240}$Pu inventories the soil core at sampling site D1

675

676

677

678

679

680

681

682

683 Table 1. The depth and rate of soil erosion, and erosion intensity in the study site

	D1	D2	D3	Y1	Y2	Y3
Total inventory of $^{239,240}Pu$ (Bq/m^2)	111	53.4	75.4	72.9	56.5	186
Soil erosion depth (cm)		4.6	2.4	2.6	4.2	-3.3
Soil erosion rate ($t/km^2/yr$)		941	538	551	845	-719
Erosion intensity		minor erosion	minor erosion	minor erosion	minor erosion	accumulation

684

685

686

687

688

689

690

691

692

693

694

695

696 Table 2. The soil erosion rate of DZG and YJG during the different time

Time	Soil erosion rate (t/km^2/yr)		Precipitation rate	Reference
	DZG	YJG	(mm)	
1954-1962	4610	1280	567	(Chen, 2010; Li, 2006; Yuan et al., 2014)
1963-2012*	3000	454	414	
1963-2016	538-941	551-845	556	This study

697 Note: *the data are not available in 1970-1971, 1978-1986 and 1995-2011

698

699

700

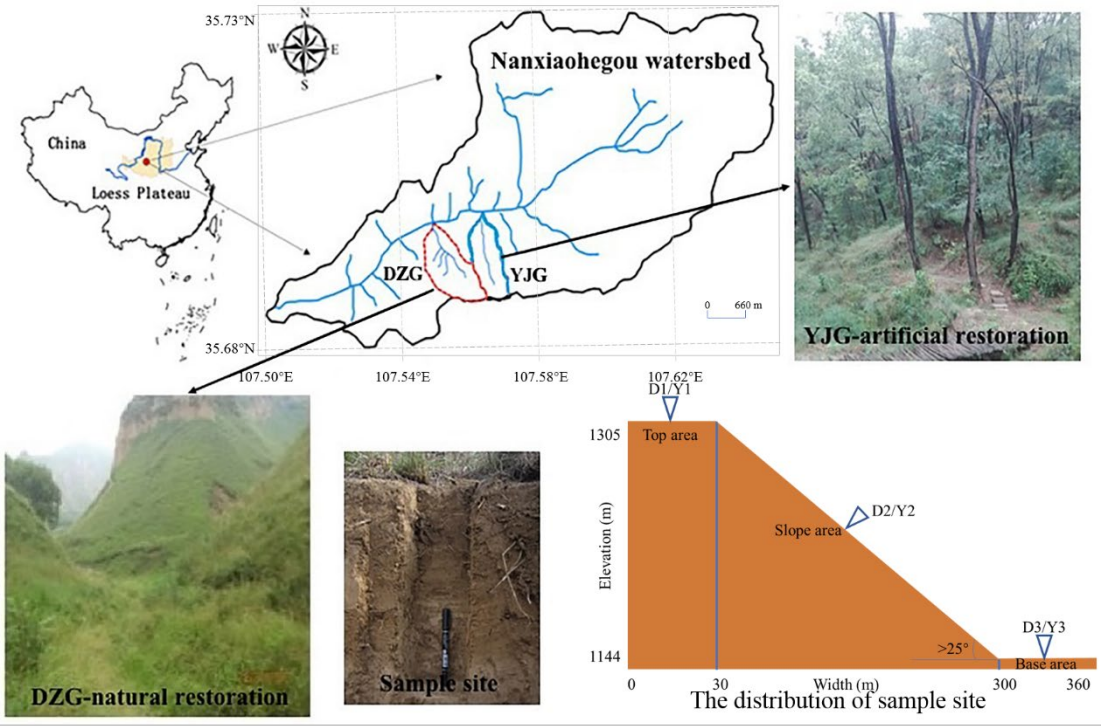

Fig. 1 Sampling sites in the DZG and YJG in Nanxiaohegou watershed in the Loess Plateau in northwest China. The elevations of the top catchments and the height from the base to the top area are 1271m and 127 m for YJG and 1305 m and 160m in DZG, the slopes of two catchments are 35° for YJG and 25° for DZG (slope of the sampling sites at slope); the distances among top-slope and slope-base sampling sites are 250 m and 100 m in YJG and 200 m and 150 m for DZG catchment.

714

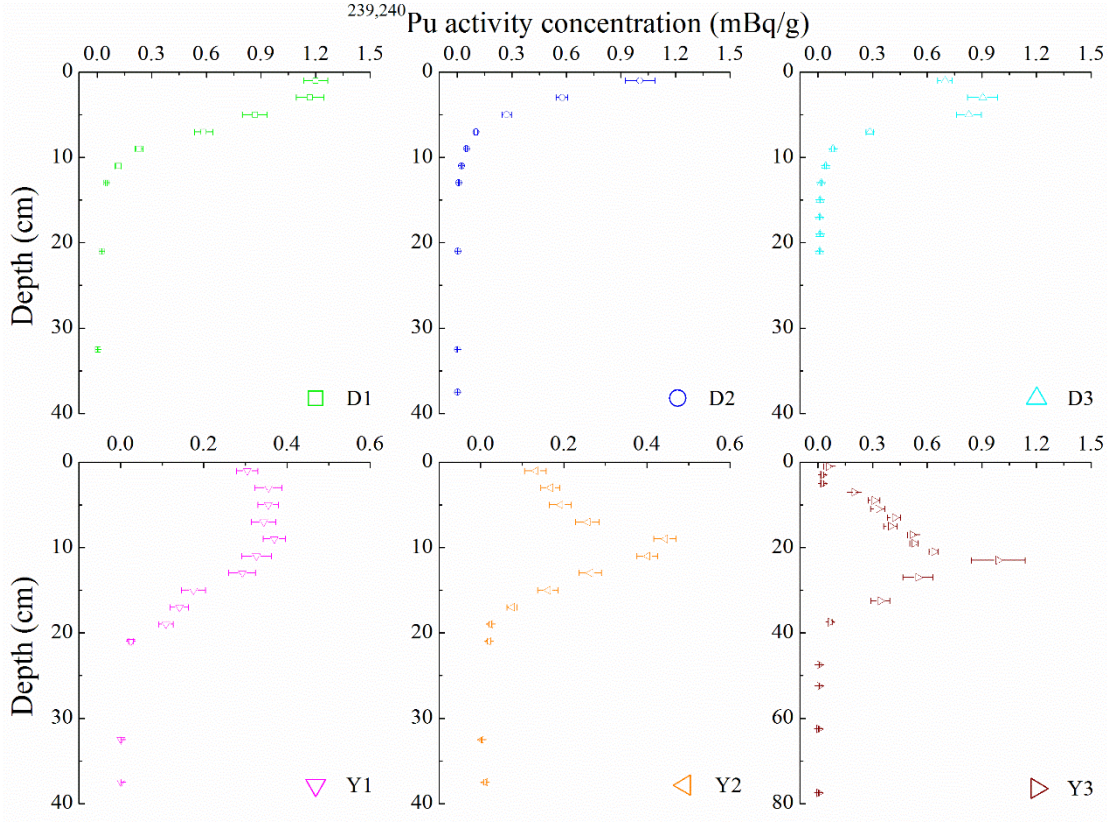

715
716
717
718 Fig. 2 Depth distributions of ^{239,240}Pu activity concentrations in six soil profiles

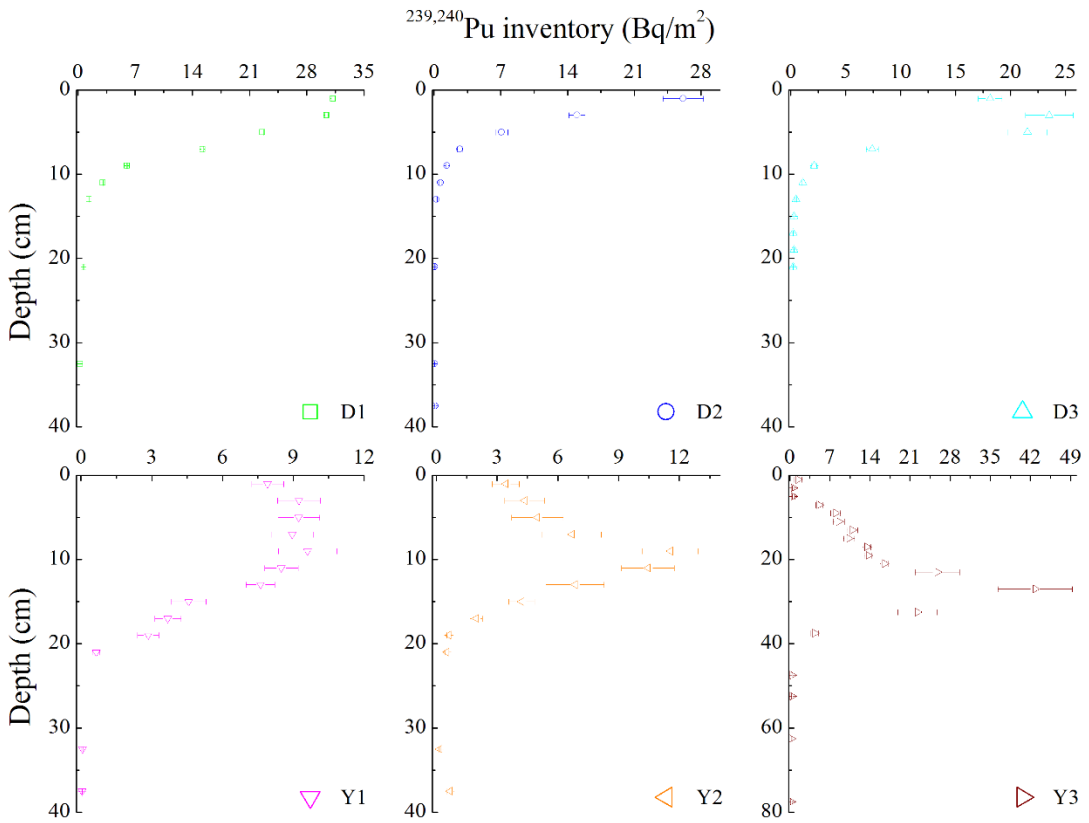

719
720
721
722 Fig. 3 Depth distributions of ^{239,240}Pu inventory in six soil profiles
723
724

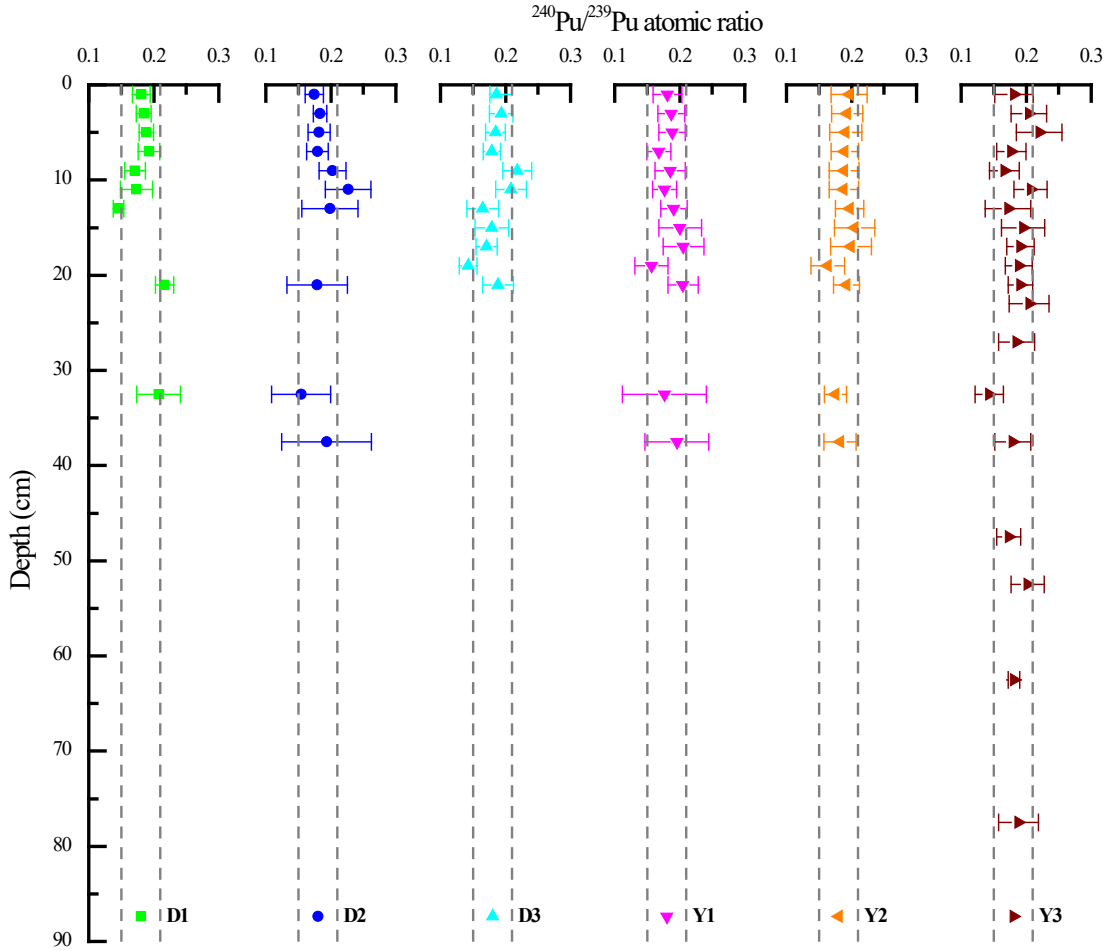

Fig. 4 Depth distributions of the $^{240}Pu/^{239}Pu$ atomic ratios in the sampling sites

734

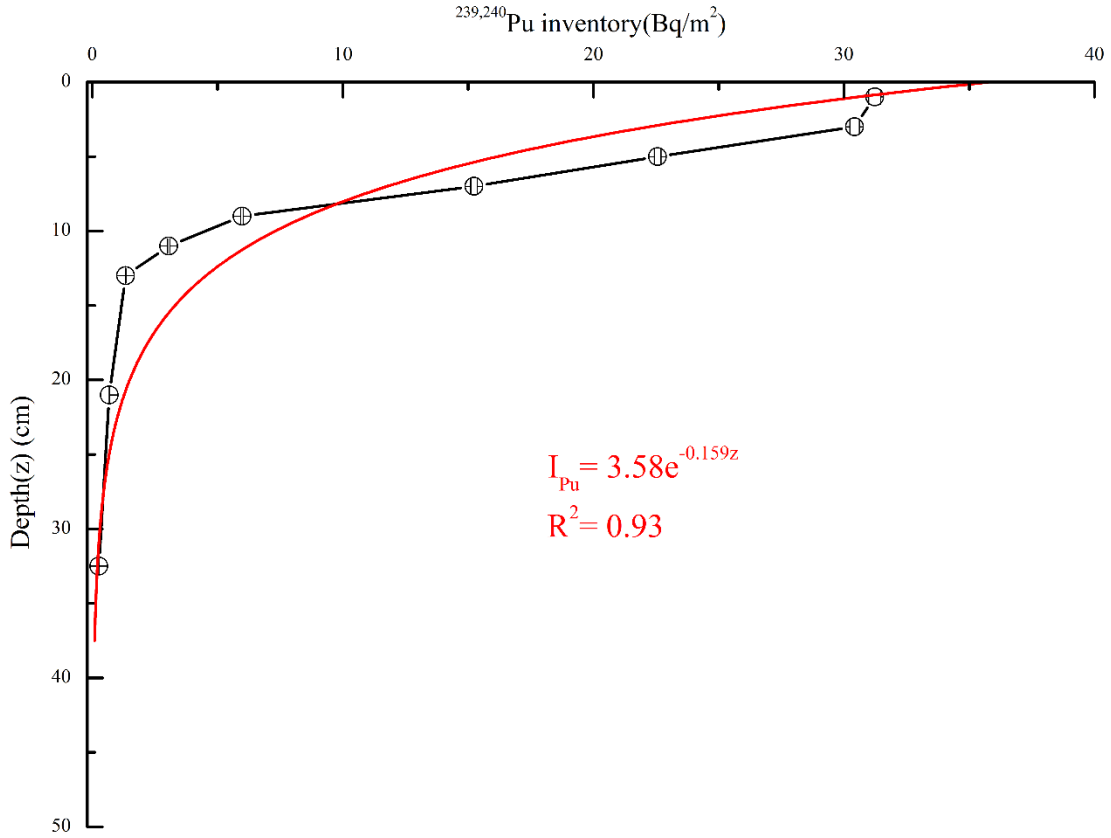

735

736

737 Fig. 5 Depth distribution of ^{239,240}Pu inventories the soil core at sampling site D1

738